Paper presented at the East Europe Conference on AM Materials (EECAM21)
September 2-4, 2021, Belgrade, Serbia

Iulian-Ionuț Ailinei, Sergiu-Valentin Galațanu, Liviu Marșavina[*]

INFLUENCE OF DEPOSITION DIRECTION ON VIBRATION CHARACTERISTICS OF 3D PRINTED ABS TEST SPECIMENS

UTICAJ PRAVCA DEPOZICIJE NA VIBRACIONE KARAKTERISTIKE 3D ŠTAMPANIH ABS UZORAKA ZA ISPITIVANJE

Originalni naučni rad / Original scientific paper
UDK /UDC:

Rad primljen / Paper received: 11.12.2021

Adresa autora / Author's address:
Mechanics and Strength of Materials, Politehnica University of Timisoara, Timișoara, Timiș, Romania
email: liviu.marsavina@upt.ro

Keywords
- ABS (acrylonitrile butadiene styrene)
- vibration
- deposition direction
- frequency response function
- additive manufacturing

Abstract

This article compares the vibrational behaviour variability of acrylonitrile butadiene styrene (ABS) test specimens obtained by additive manufacturing (AM) with three different deposition directions.

Test specimens are subjected to forced vibration on an electromechanical shaker, and the frequency response amplitude is measured using accelerometers. Natural frequency and Q-factors are discussed.

The experiment shows that the direction of deposition generates a material damping variability of up to 30 %. The parameters identified during experiments could be further used to develop finite element numerical models to virtually validate 3D printed structures generated with the same process parameters as the test samples.

Ključne reči
- ABS (akrilonitril butadijen stiren)
- vibracije
- pravac depozicije
- funkcija frekventnog odziva
- aditivna proizvodnja

Izvod

U ovom radu je dato poređenje promenjivog ponašanja vibracija ispitnih epruveta od akrilonitril butadijen stirena (ABS), dobijenih aditivnom proizvodnjom (AM) u tri različita pravca depozicije.

Epruvete za ispitivanje su podvrgnute vibracijama na elektromehaničkom uređaju, zatim se meri amplituda frekventnog odziva primenom akcelerometara. Data je diskusija o sopstvenim frekvencijama i Q-faktora.

U eksperimentu se sa pravcem depozicije generiše promenljivo prigušenje u materijalu do 30 %. Parametri koji se određuju u eksperimentima se mogu dalje iskoristiti za razvoj numeričkih modela sa konačnim elementima kako bi se virtuelno ocenilo ponašanje 3D štampane konstrukcije generisane sa istim parametrima kao i ispitivane epruvete.

INTRODUCTION

Additive manufacturing is a general term for manufacturing technologies that rely on adding (not subtracting) layers of material, following a digital object that must be manufactured /1-5/. The method offers many advantages, like mass customization (very appealing for noise vibration and harshness management), reduced tooling costs, reduced delivery time (suitable for rapid prototyping) and reduced material waste by topology optimisation /6-8/. Despite the many advantages, the material properties, both for static and dynamic loading, depending on process parameters, and datasheet values are inaccurate or do not contain critical parameters like infill percentage or part orientation, /9/.

AM technologies demonstrate huge promise and may revolutionize design, manufacturing, logistics, maintenance and acquisition in real-world scenarios. However, there are still multiple hurdles to overcome before AM becomes an efective component in the industry toolset, /10/.

Vibration properties such as frequency, deflection and damping of the FDM printed part are investigated in /11/. The natural frequency of the beam obtained from experiment on keep observation indicates the fact that the value changes when the layer orientation and layer thickness of the beam changes.

The characterization of the properties of ABS parts fabricated by the FDM 1650 are investigated in /12/. Using a Design of Experiment (DOE) approach, the process parameters of FDM, such as raster orientation, air gap, bead width, colour, and model temperature are examined. The typical tensile strength ranges between 65 and 72 % of the strength of injection molded ABS P400. The compressive strength ranges from 80 to 90 % of the injection molded FDM ABS.

The results of the fused deposition modelling samples indicate lower variation between designed and printed dimensions compared to stereolithographic samples, which is likely due to the larger size of the FDM samples /13/. The percent difference in quality factor with and without vacuum for the FDM samples is less than 5 % for most of the materials, indicating low sensitivity to fluid damping.

Vibration damping capabilities of sleeve bearing printed from PA12 (nylon) filament material using Fused Deposition Modelling (FDM) method is experimentally analysed in /14/. Filling structures and occupancy rates have a very important role in the damping capabilities of sleeve bearings.

The objective of this paper is to determine frequency response functions (FRF) experimentally, natural frequencies experimentally and to calculate Q-factors /15, 16/ for each deposition direction in order to explore the vibrational behaviour of ABS specimens obtained by additive manufacturing, also known as 3D printing in colloquial language.

The previously determined parameters should be used to compute the natural frequencies using the finite element method.

EXPERIMENTAL INVESTIGATIONS

For this study, standard test specimens (Fig. 1) are used according to DIN ISO-20753 /17/ of details as depicted in Table 1.

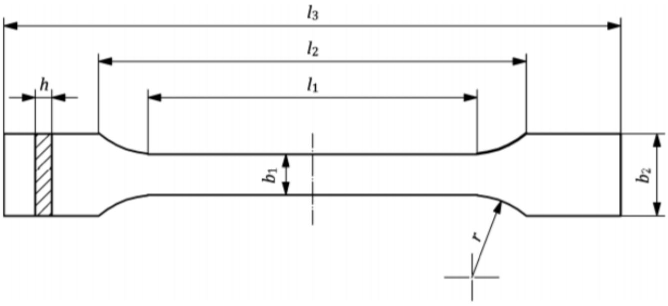

Figure 1. ISO 20573 tensile specimen.

Table 1. Dimensions of the test specimen.

Dimension	Value (mm)
l_1	70
l_2	10
l_3	150
b_1	10
b_2	20
h	4
r	35

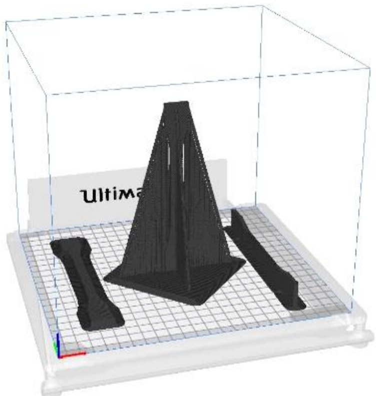

Figure 2. Specimens orientation.

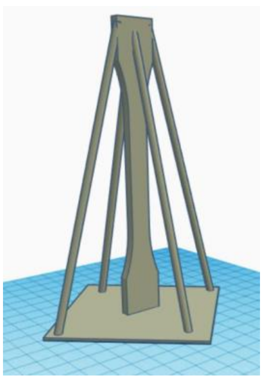

Figure 3. Support structure for ZX specimen.

Fabrication of specimens is done using an Ultimaker 3, 3D printing machine, which has dual extrusion with a build volume of 230×190×200 mm, down to 20 μm (0.001 in.) layer resolution, open filament system, compatible with glass and carbon fibre composites, with dual filament flow sensors. The most critical parameters that significantly influence sample quality and printing duration are the percentage of infill and printing resolution. An infill percentage of approximately 100 % is chosen to have a uniform mass inside the specimens, and printing resolution is chosen at a 0.2 mm linear increment to decrease the printing time. Figure 2 shows the printer setup and orientation of the test specimen.

To compare the anisotropy generated by the deposition direction, three samples are printed in the same setup, one sample laying on the XY plane, the second in the YZ plane, and the third in the ZX plane, as in Fig. 2. To ensure the printability of the ZX specimen, special supports are added so that they do not influence the gauge length of the specimen (Fig. 3). Total duration time of printing was 8.5 hours.

Test setup

An electrodynamic shaker is used to generate forced harmonic motion to excite the test specimens. Piezo-electric accelerometers are used to measure the acceleration response during the vibration test. A broadband sine sweep vibration profile is used ranging from 10 to 1000 Hz, with a constant acceleration of 1 G, having a linear sweep rate of 1 Hz/s over the entire spectrum. Complete vibration test setup can be observed in Fig. 4, where (1) represents the fixture that clamps the specimen (2). The setup is controlled by the drive acceleration sensor (3), and sensor (4) measures the acceleration response of the test sample. Three runs were made, one for each test sample.

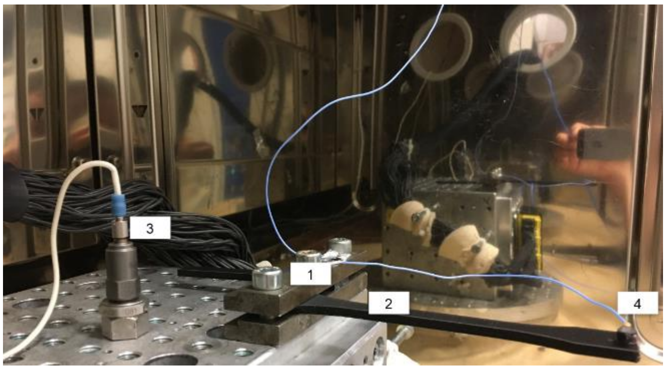

Figure 4. Vibration test setup.

RESULTS AND DISCUSSION

Failures due to vibration loads are caused by the maximal G loads experienced by the device under test (DUT).

Most products have resonance frequencies in the testing range. Resonant frequencies, transmissibility and Q-factor are determinate factors in vibration-induced failures. These are depicted in Fig. 5.

A product is subjected to fatigue loading when exposed to its natural resonance /18/. The transmissibility of a resonance refers to the ratio of the input acceleration to the response acceleration.

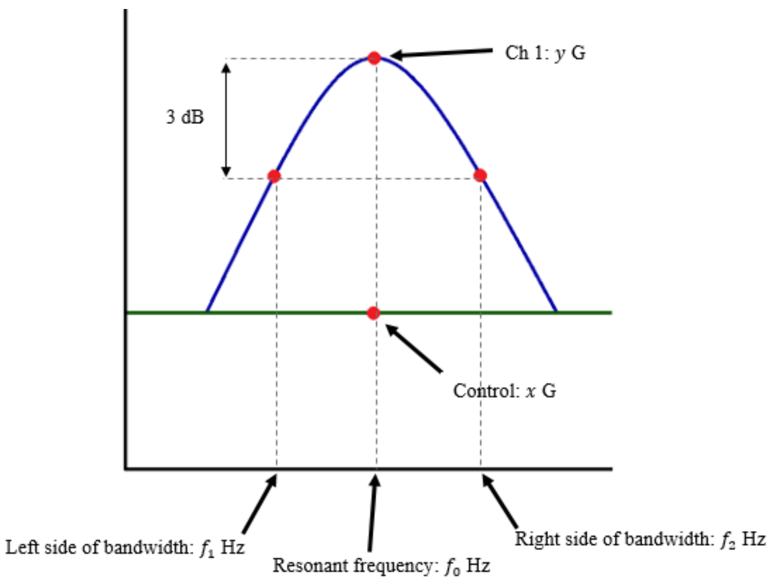

Figure 5. Q-factor calculation.

The resonance bandwidth is computed as the distance in Hz between the 3 dB drop-offs on each side of the resonance. This is also known as the half-power bandwidth method /19/. The Q-factor of resonance is defined as the ratio of the centre frequency of the resonance and the half-power bandwidth of the resonance. The Q-factor shows how sharp or steep a resonance is.

$$Q_{factor} = \frac{\text{resonant frequency}}{-3\text{db bandwidth (BW)}} = \frac{f_0 \text{ (Hz)}}{f_2 \text{ (Hz)} - f_1 \text{ (Hz)}} . \quad (1)$$

Damping is an energy dissipation mechanism that causes vibration to diminish over time and eventually stop /20/. The vibrational energy is converted into sound or heat. The amount of damping depends on the material, the velocity of motion, and the vibration frequency. Structural damping ξ is linked to the Q-factor via:

$$\xi = \frac{1}{2Q} . \quad (2)$$

In Fig. 6, the frequency response functions for the three runs are plotted. From this log-log plot, one can observe no significant difference between the frequency response function, except that the samples ZX results are left-shifted, showing the lower stiffness. To have a deeper inside, the values of resonant frequencies, response amplitudes, and Q-factors are normalized to sample XY for better emphasis on variance of anisotropy generated by the deposition direction.

In Fig. 7, normalized resonant frequencies are shown. All samples have three resonant frequencies in the testing range of 10 to 1000 Hz. From this chart, one can conclude that sample XY is the most rigid, and other samples have a significant drop in stiffness, almost 40 %. In the other modes, the drop is consistent, but not significant, up to 3 and 7 %.

In Fig. 8, the normalized amplitudes are shown. One can observe that amplitudes are also dropping, with sample XY having the largest amplitudes, the sample YZ medium, and the sample ZX having the smallest.

This tendency is not shown for the second resonant frequency. This could be clarified by running more tests.

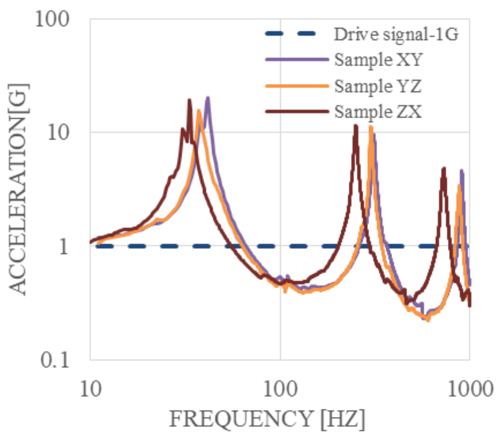

Figure 6. Frequency response functions.

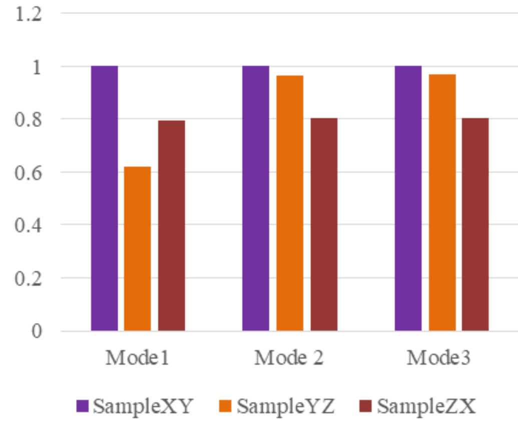

Figure 7. Normalized resonant frequencies.

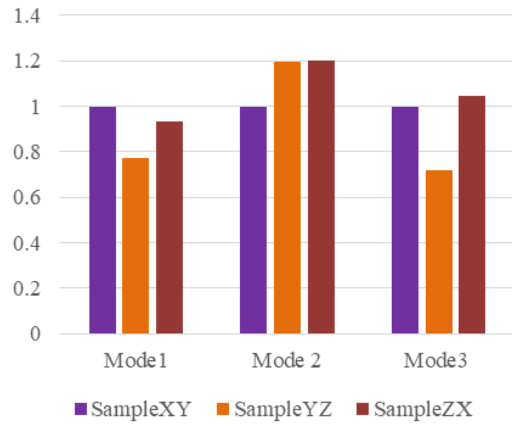

Figure 8. Normalized frequency responses.

Q-factors are shown in Fig. 9. The tendency of Q-factors to decrease over frequency is kept. The change in deposition direction has a similar effect. Since the Q factor gives an inside of the damping behaviour, one can observe that the predominant type of damping is the viscous one (proportional to velocity or frequency of the structure) like in polymers obtained by other manufacturing methods as injection moulding or extrusion. That means the damping can be modelled in FEA analyses with ease.

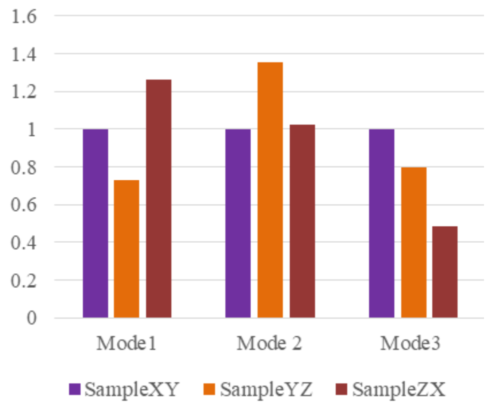

Figure 9. Normalized Q-factors.

CONCLUSIONS

This study explores the vibrational behaviour of ABS test specimens fabricated by additive manufacturing, with three different deposition directions.

The vibration measurement shows that the anisotropy generated by the deposition direction has the most significant influence on Q-factor, resulting in variations of the viscous damping of up to 30 %.

Future efforts should be directed toward generated finite element models that incorporate the anisotropy generated by the deposition direction.

By performing more test runs to ensure the statistical meaning of the experimental data, the anisotropy generated by the deposition direction can be estimated and incorporated in finite element models (beyond the scope of this paper) and then used in the vibration design of 3D printed industrial products.

ACKNOWLEDGEMENTS

The project leading to this application has received the funding from the European Union's Horizon 2020 research and innovation program under grant agreement No 857124.

REFERENCES

1. Ezeiruaku, S. (2016), Review of additive manufacturing and characterization of additive manufacturing machines, Master’s Thesis, University of New Mexico, Albuquerque, New Mexico, USA. doi: 10.13140/RG.2.1.3630.6009
2. Lifton, V., Lifton, G., Simon, S. (2014), *Options for additive rapid prototyping methods (3D printing) in MEMS technology*, Rapid Prototyp. J, 20(5): 403-412. doi: 10.1108/RPJ-04-2013-0038
3. Swanson, W.J., Johnson, K.C., Hjelsand, T.A., Batchelder, J.S., Method for building three-dimensional models with extrusion-based additive manufacturing systems, Patent: US8815141B2, 2014.
4. Niesler, F.B.P., Hermatschweiler, M. (2014), *Additive manufacturing of micro-sized parts*, Laser Technik J, 11(5): 16-18. doi: 10.1002/latj.201400048
5. Korpela, M., Riikonen, N., Piili, H., et al., Additive Manufacturing - Past, Present, and the Future, In: Collan M., Michelsen KE. (Eds.), Technical, Economic, and Societal Effects of Manufacturing 4.0., 2020, Palgrave Macmillan, Cham. doi: 10.1007/978-3-030-46103-4_2
6. Attaran, M. (2017), *The rise of 3-D printing: The advantages of additive manufacturing over traditional manufacturing*, Bus. Horizons, 60(5): 677-688. doi: 10.1016/j.bushor.2017.05.011
7. Lacroix, R., Seifert, R.W., Timonina-Farkas, A. (2021), *Benefiting from additive manufacturing for mass customization across the product life cycle*, Oper. Res. Perspectives, 8: 100201. doi: 10.1016/j.orp.2021.100201
8. Montero, D.S., Silva, O.M., Cardoso, E.L. (2020), *Topology optimization for harmonic vibration problems using a density-weighted norm objective function*, Struct. Multidisc. Optim. 62: 3301-3327. doi: 10.1007/s00158-020-02695-0
9. Dudescu, C., Racz, L. (2017), *Effects of raster orientation, infill rate and infill pattern on the mechanical properties of 3D printed materials*, Acta Universitatis Cibiniensis, Tech. Ser. 69(1): 24-30. doi: 10.1515/aucts-2017-0004
10. Vora, H.D., Sanyal, S. (2020), *A comprehensive review: metrology in additive manufacturing and 3D*, Prog. Addit. Manuf. 5: 319-353. doi: 10.1007/s40964-020-00142-6
11. Chaitanya, S.K., Reddy, K.M., Ch, S.N.S.H. (2015), *Vibration properties of 3D printed/rapid prototype parts*, Int. J Innov. Res. Sci. Eng. Technol. 4(6): 4602-08 doi: 10.15680/IJIRSET.2015.0406087
12. Ahn, S.-H., Montero, M., Odell, D., et al. (2002), *Anisotropic material properties of fused deposition modeling ABS*, Rapid Prototyp. J. 8(4): 248-257. doi: 10.1108/13552540210441166
13. Gietl, J., Vignola, J., Sterling, J., Ryan, T. (2018), *Characterization of damping properties in 3D printed structures*, J Phys.: Conf. Ser. 1149 012002. doi: 10.1088/1742-6596/1149/1/012002
14. Kam, M., Saruhan, H., İpekci, A. (2021), *Experimental analysis of vibration damping capabilities of sleeve bearings printed using FDM method*, J Polytech. doi: 10.2339/politeknik.643842
15. Bird, J., Chapter 32: Parallel Resonance and Q-factor, In: Bird's Electrical Circuit Theory and Technology, 7th Ed., Routledge, London, 2021. doi: 10.1201/9781003130338
16. Zollner, M., Zwicker, T. (2019), Factoring in the Q, GITEC Knowledge Base: Q-Factor and Damping, Tech. Rep. doi: 10.13140/RG.2.2.22403.66085
17. ISO 20753: 2018 Plastics-Test specimens, Berlin, 2018.
18. Moon, S-I., Cho, I-J., Yoon, D. (2011), *Fatigue life evaluation of mechanical components using vibration fatigue analysis technique*, J Mech. Sci. Technol. 25(3): 631-637. doi: 10.1007/s12206-011-0124-6
19. Carmichel, S., Estimating Damping Values Using the Half Power Method, Integrated Systems Research, Inc., Tech Brief 150401 D, 2015.
20. Silas, Gh., Mecanica. Vibratii Mecanice, Ed. Didactica si Pedagogica, 1968 (in Romanian)